Iranian Journal of Materials Forming

Research Article

Production of Al5083-Al₂O₃ Metal Base Composite Using Accumulative Roll Bonding

M. Jafari[1], S.M.H. Seyedkashi[1*], M. Elyasi[2] and Y. Yaghoubinezhad[3]

[1] Department of Mechanical Engineering, University of Birjand, Birjand, Iran
[2] Faculty of Mechanical Engineering, Babol Noshirvani University of Technology, Babol, Iran
[3] Department of Mechanical and Materials Engineering, Birjand University of Technology, Birjand, Iran

A R T I C L E   I N F O

A B S T R A C T

The strength of aluminum Al5083 laminated composite in accumulative roll bonding (ARB) is increased using Al₂O₃ nanoparticles. For this purpose, the ARB process was conducted at room temperature without lubricants in four consecutive passes. A thickness reduction of 50% in each pass was considered with no heat treatment between sequential passes. In each pass, Al₂O₃ nanoparticles were placed between the layers. Finally, the produced metal composite was evaluated for microstructural and mechanical properties using optical microscopy, and uniaxial tensile, microhardness, and peeling tests according to the relevant standards. The primary objective of this research was to enhance the tensile strength of the composite after work hardening by incorporating nanoparticles and annealing in the final cycle. The results showed that with an increase in accumulative roll bonding cycles, tensile strength and hardness increased, and this increase occurred more prominently in the initial cycles. Furthermore, the amount of elongation decreased at the end of the first pass and then increased until the end of the fourth pass. These changes in mechanical properties during the ARB process are due to the dominant mechanisms of work hardening and strain hardening in the initial cycles and the improvement in microstructure and refinement of grains in the final cycles of this process. The highest tensile strength and microhardness, which increased by 48.1% and 55.9%, respectively, compared to the initial sample were measured at the end of the fourth cycle. Additionally, comparing the heat-treated sample with Al₂O₃ nanoparticles to the base metal showed a 34.9% increase in strength and a 30.8% decrease in elongation.

© Shiraz University, Shiraz, Iran, 2024

1. Introduction

In recent years, metallic composites have received more attention in industrial applications, and various methods have been utilized to produce these types of metallic composites. Layered aluminum alloys and composites are increasingly used in the automotive industry for heat transfer applications due to several favorable properties, such as low density, desirable mechanical properties, good thermal conductivity, and relatively good corrosion resistance [2]. On the other hand, in recent years, investigating methods for producing and studying the mechanical properties of

---

materials with nano-sized grains or very fine grains has been the subject of much research in the field of materials and related sciences. These materials, known as "Super Metals" exhibit unique properties such as high strength at ambient temperatures, superplasticity at high temperatures, low strain rate sensitivity, and excellent corrosion resistance [3].

Generally, the manufacturing of these materials falls into two categories: top-down and bottom-up approaches. One of the most widely used methods for fabricating materials with fine structures is severe plastic deformation (SPD) which belongs to the top-down category [4]. Severe plastic deformation processes are one of the most suitable methods for producing metallic materials with micro and nano grain sizes on an industrial scale [5, 6]. In all of these methods, the crystals inside the metals are subjected to high pressure and exposed to high shear stress, resulting in a metal grains size reduction of. The common and unique feature of these processes is the constant dimension of the initial sample during the process, which eliminates the limitations on applying strain and facilitates achieving very high strains in the material. Consequently, the application of strain allows for the refinement of the microstructure, reducing the grain size to the nanoscale, and improving the mechanical properties of the metallic sample while maintaining its initial geometry [7]. Various processes have been used for severe plastic deformation of metals, such as equal channel angular pressing (ECAP) [8], cyclic extrusion and compression [9], and high-pressure torsion [10]. In these processes, maintaining the sample dimensions is a common feature, enabling the application of extremely high shear strains. However, the production rate is low in these processes. Moreover, in most cases the use of high-capacity forming machines and expensive dies is necessary. Among these processes, accumulative roll bonding has been successfully applied to many metallic materials. In 1998, Saito and Utsunomiya invented a new method called accumulative roll bonding (ARB) [11, 12]. They stated that this method is one of the most important

severe plastic deformation methods that introduces large plastic strains into the sheet without changing its dimensions and leads to the formation of an exceptionally fine-grained structure that improves its mechanical properties.

In the ARB process, a sheet that has been thinned by rolling is cut into two parts, and then these two sheets are stacked and rolled again [13, 14]. Since the mentioned stages in this process can be repeated without limitation until the material undergoes significant work hardening, there is the potential to apply very large plastic strains to the material [15, 16]. The accumulative roll bonding process has been successfully applied to materials such as similar aluminum [17], steel [18], and pure copper [19], as well as dissimilar materials like aluminum-copper [20] and aluminum-titanium [21], resulting in the formation of ultrafine microstructures and high strength in all cases. Severe plastic deformation applied by the accumulative roll bonding process to metals and similar alloys leads to grain refinement due to the formation of high-angle grain boundaries and low-angle grain boundaries, ultimately forming structures with ultrafine grains and equiaxed grain boundaries [22]. Sedighi et al. [23] investigated the effect of alumina content on the mechanical properties of AA5083/Al_2O_3 composites fabricated through hot accumulative roll bonding. Their results indicated that with an increase in alumina content, the tensile strength and hardness of the composites increased, whereas their elongation decreased. The microstructure of the composites showed that alumina particles were uniformly distributed within the aluminum matrix, and with higher alumina content, the grain size decreased. The difference between our study and that of Sedighi et al.'s [23] lies in the use of cold accumulative roll bonding and the amount of alumina used. Mosleh-Shirazi et al. [24] investigated the effects of nano-sized silicon carbide (SiC) content on the hardness, dry sliding wear, corrosion, and erosive wear of Al/SiC nanocomposites synthesized by mechanical milling. Their findings showed that increasing the SiC content led to an

increase in the hardness of the nanocomposites. The observed enhancement in corrosion resistance of Al/SiC nanocomposites with their SiC content was attributed to the fact that nano-SiC particles do not chemically react with the corrosive solution. Al/SiC nanocomposites exhibited superior wear resistance and lower friction coefficient compared to the base metal in both dry and corrosive environments. Akhlaqi et al. [25] investigated the tribological behavior of Al/SiC and Al/SiC/2vol.%Gr nanocomposites containing different amounts of SiC nanoparticles. They demonstrated uniform distribution of the reinforcing particles in the nanocomposite matrices using SEM and TEM studies. Although increasing the SiC content led to an increase in the hardness of both Al/SiC and Al/SiC/2vol.%Gr nanocomposite series, all Al/SiC/2vol.%Gr composite specimens exhibited lower hardness than their Al/SiC counterparts with the same SiC content. Furthermore, increasing the SiC content resulted in a decrease in wear rate and friction coefficient for both Al/SiC and Al/SiC/2vol.%Gr nanocomposite series. The presence of Gr led to abrasive wear and delamination for Al/SiC/2vol.%Gr nanocomposites.

The literature review on various materials indicates an improvement in mechanical properties, such as an increase in strength up to three to four times. However, this increase in strength has been more pronounced in aluminum alloys. The use of metals such as steel and titanium requires equipment with higher cost and power due to their high initial strength [26, 27]. Commonly, high hardness of alumina particles makes it a desirable additive for utilizing as an emergent reinforcement in aluminum base composites [28-31].

The literature review shows that the production of high-strength aluminum is one of the demands of industries. On the other hand, increasing the strength of metals without a significant decrease in ductility has always been a perennial challenge in forming processes. In this study, by employing nanoparticles between the layers of aluminum sheets in the accumulative roll bonding process at room temperature, a composite metal with significantly higher strength and acceptable ductility compared to the base metal has been produced. The mechanical properties of the investigated composites are further discussed.

2. Materials and Methods

The mechanical properties of aluminum 5083 used in this study are shown in Table 1. Generally, this metal has high weldability and good post-weld strength. Before the accumulative roll bonding operation, the samples were subjected to the annealing heat treatment. Annealing was carried out for one hour at a temperature of 400 °C in a furnace, and then the furnace was turned off and cooled and along with the samples.

Table 1. Mechanical properties of Al5083

Grade	UTS (MPa)	Yield strength (MPa)	Elongation (%)	Hardness (HV)
AA5083	293	145	29	26.3

In the accumulative roll bonding process, the 2 mm thick sheets were cut perpendicular to the rolling direction into dimensions of 100 mm in length and 40 mm in width. Subsequently, two pieces were degreased using a solvent and abraded with a steel brush to remove the surface oxide layer. Based on Fig. 1, two sheets were placed together, and Al_2O_3 nanoparticles (13 nm) were inserted between the sheets at a rate of 0.75 g/cm² as a reinforcement. To prevent delamination and slipping of the layers, holes were drilled at four corners of the stacked layers and they were tightly bound together using steel wire. As shown in Fig. 2(a), a Sahinler rolling mill with roller diameters of 250 mm was used. Then, accumulative roll bonding with a 50% thickness reduction at each pass was applied. To ensure data reliability, each test was repeated three times.

For mechanical property evaluation, tensile tests were conducted at room temperature using a SANTAM S20 universal tensile and compression testing machine. Tensile test specimens were prepared according to ASTM E8/E8M standard along the rolling direction.
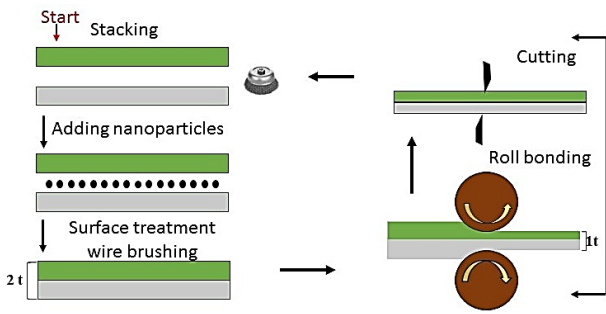
Fig. 1. Accumulative roll bonding process.

After the tensile test, stress-strain curves were plotted for the ARB specimens after different cycles. The elongation of the specimens was determined by measuring the gauge length before and after the tensile test. In order to measure the hardness of the samples, a Vickers hardness tester with a load of 5 kg was used for 10 to 15 seconds perpendicular to the rolling direction. As shown in Fig. 2(b), three specific points on the bonding interface were selected at equal distances after the fourth cycle, and their hardness was measured. Then, the average of these points was reported as the
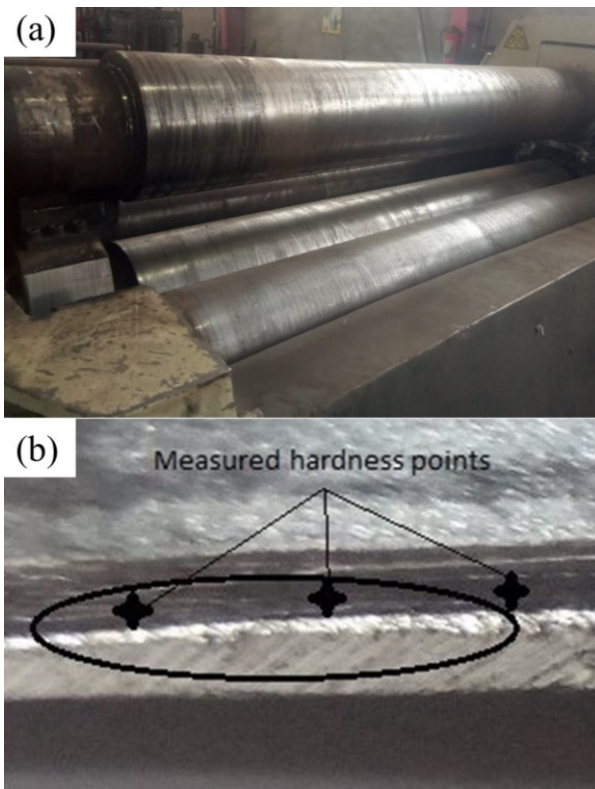
hardness value. To obtain the shear force of the sheets for the adhesion test, a peel adhesion test was used.

To investigate the sample using XRD analysis and utilize its advantages in chemical analysis and crystallographic aspects, an ultrasonic device with Panasonic model 2600 specifications was employed. The device operated with an applied voltage of 220 V, a frequency of 50 Hz, and a power of 50 W to partially disintegrate the nodes and lumps.

3. Results and Discussion

Initially, to investigate the reliable number of accumulative roll bonding cycles in this study, the cycles were increased and studied from one cycle upward. Fig. 3 shows the rolled piece after five cycles. The results showed that after five cycles, the sheets cracked due to excessive strain and were neither assessable nor usable. Therefore, in the subsequent experiments, the sheets were only rolled up to four cycles.

The number of layers of the ARBed sheet is equal to 2^n, where n is the number of cycles. Hence, the sheet rolled for 4 cycles has 16 layers, and the thickness of each layer is 125 μm. With a 50% thickness reduction at each cycle, the total thickness reduction of each layer after four cycles is 93.75%. To increase adhesion, this process was performed under non-lubricated conditions which resulted in severe plastic deformation. As shown in Fig. 4, the ultimate tensile strength of the annealed sheet was 313.8 MPa, which
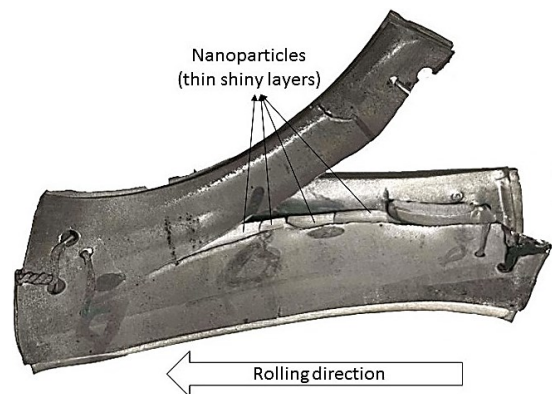

Fig. 2. (a) Sahinler roll machine and (b) measured hardness points.

Fig. 3. A defect in the ARB process on the sheet in the form of a longitudinal crack after 5 cycles.

increased to 418.7 MPa after the first cycle of accumulative roll bonding. This increasing trend continued in subsequent cycles as well. Consequently, the ultimate tensile strength increases with the number of cycles, while the amount of elongation reduction in the sheet decreases. An important factor in this increasing trend is the increase in work hardening at each stage of the rolling cycle, which reduces the grain size of the sheet while decreasing its thickness leading to increased strength.

After the annealing process was completed, the average grain size in the aluminum was 32 nm, and it decreased to 31, 28, 25, and 20 nm after the first, second, third, and fourth cycles, respectively. This indicates an increase in elongation at each cycle of the process and the development of work hardening in the final cycles. Fig. 5 compares the engineering stress-strain curves obtained for ARBed samples from one to four cycles and the base metal. According to these results, the tensile strength using nanoparticles (0.75 grams per square centimeter) was 478.76 MPa, while without nanoparticles, it was 432.12 MPa, which is 10% higher than the sample without nanoparticles. Two mechanisms of strain hardening and primary grain strengthening have led to an increase in tensile strength in the accumulative roll bonding process. Nanoparticles have caused the layers to slide over each other. The density and localized strain hardening of these areas increased with the increase in nanoparticles. According to Fig. 5 and Table 2, adding alumina has reduced the elongation of the samples. This reduction can be attributed to the weakness of the accumulation of Al_2O_3
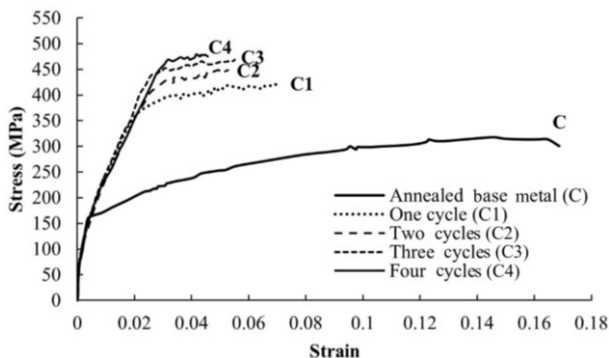
nanoparticles in the metal matrix. On the other hand, nanoparticles between the layers have voids that affect the reduction in elongation. The hard nanoparticles prevent the movement of dislocations and lead to the accumulation of dislocations around the alumina particles [32]. On the other hand, by comparing the curves, it is observed that the produced metal composite has high strength while maintaining its ductility to a considerable extent.

In Fig. 6, graphs showing changes in yield strength, ultimate tensile strength, and strain in different cycles are presented. The results show that with an increase in the cycles of the accumulative roll-bonding process, a more uniform structure with a stronger bond is created. The highest tensile strength and yield strength for the produced sample are 477 MPa and 468 MPa, respectively, which are obtained after the fourth cycle. These values are more than twice that of the annealed sample. The increase of elongation in the final cycles, especially compared to the initial cycles, is due to the reduction of the effect of strain hardening in the higher cycles and the grain refinement mechanisms in the final cycles, leading to the improved microstructure. As observed in this figure, at the end of the first ARB cycle, strength increased significantly, followed by a decrease in elongation. The main reason for this phenomenon is the increase in dislocation density due to strain hardening, high strain rates, and cold work, which are prominent mechanisms in the initial cycles of the process. In the subsequent cycles, with an increase in the ARB cycles, tensile strength, and elongation increased with a lower rate and slope
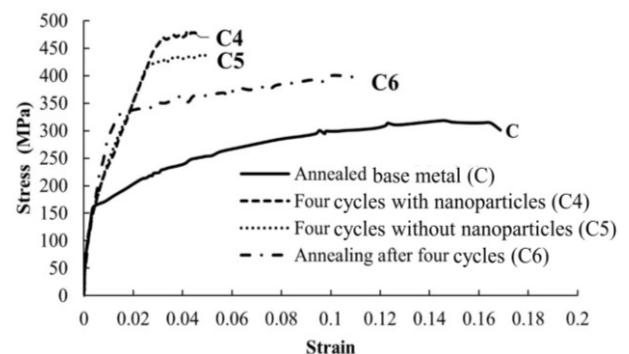

Fig. 4. Main results of tensile test experiments in different cycles using nanoparticles (0.75 g/cm²).

Fig. 5. The tensile test results after each cycle with 0.75 g/cm² nanoparticles between each layer.
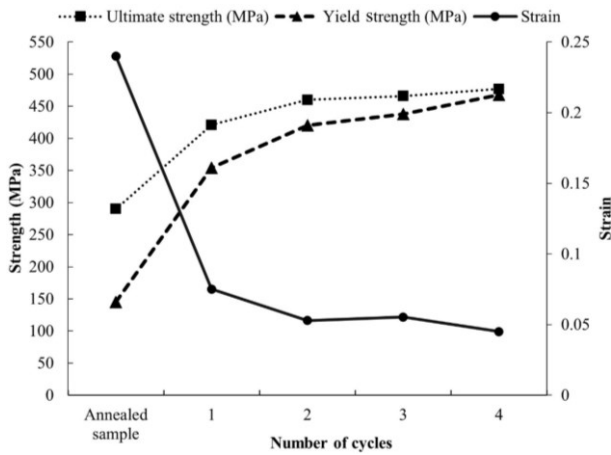
Fig. 6. Changes in tensile strength, yield stress, and strain during the accumulative rolling process.

compared to the first cycle, primarily due to grain refinement and reduced strain hardening effects [33]. Therefore, it can be concluded that the increase in strength and improvement in mechanical properties result from two mechanisms: strain hardening and grain refinement. Strain hardening predominates in the initial cycles of the process, while grain refinement plays a significant role in the subsequent cycles. Although strain-hardening effects are still observable in the final cycles, they diminish due to the increase in dislocation density saturation with the increase in ARB cycles.

In Table 2, a comparison of yield stress, ultimate tensile stress, and elongation percentage for annealed base metal samples, ARBed metal composite in 4 cycles with and without nanoparticles, and heat-treated ARBed composite with nanoparticles are presented. The obtained values show a significant increase in both yield stress and ultimate tensile strength in all cases compared to the annealed base metal. Additionally, the elongation percentage in all samples has decreased compared to the annealed base metal. Comparing the yield stress of the annealed base metal sample and the

sample annealed with nanoparticles after 4 cycles, it is observed that the yield stress has increased by approximately 91%, and the ultimate tensile stress has increased by about 27%. The reduction in elongation in this case was approximately 8.30%. Overall, this result indicates that if ARBed samples with nanoparticles are heat-treated after 4 cycles, the produced metal composite will have a 91.8% higher yield strength and approximately 31.2% lower elongation compared to the base metal. Therefore, in terms of application, a material with acceptable strength and elongation percentage is produced.

Fig. 7 depicts SEM images of specimens conducted with four cycles and three cycles. It is observed that as the cycles increase, the alignment of the aluminum layers becomes more uniform and homogeneous. In Fig. 7(b), the proper bonding interface between the sheets using nanoparticles is seen. It is observed from the images of the sheet interfaces that no porosity or cracks have been created between the layers. Additionally, the more uniform distribution of alumina nanoparticles, which act as reinforcing agents, indicates that with increasing strain and applied force, the reinforcing metal layers can become finer in the background, and their distribution becomes more uniform as the process continues. Finally, the SEM image at the interface of four cycles shows that this sample is composed of 16 layers, with each layer having an approximate thickness of 157 µm. As previously mentioned, the theoretical thickness of each layer would be 125 µm, but it is slightly different due to the nonuniform deformation of layers. Examination of the microstructure of this composite indicates that the aluminum grain size is approximately 80 nm.

Table 2. Comparison of ultimate strength, yield strength and elongation of each sample

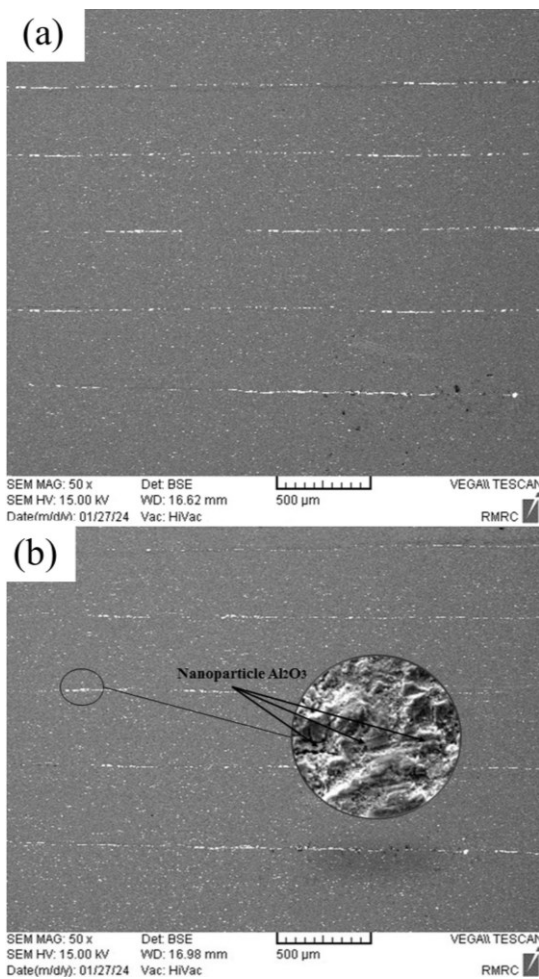| Type	Ultimate strength (MPa)	Yield strength (MPa)	Elongation%
Annealed-base metal (C)	313.778	172	24
4th cycle without nanoparticle (5)	438.355	414	7
4th cycle with nanoparticle (C4)	477.574	465	5
Annealing after 4th cycle (C6)	399.85	330	16.4
Percentage difference between C and C6	27.4% increase	91.8% increase	31.6% reduction

Fig. 7. SEM sample of aluminum layers in ARB process using nanoparticles (a) after four cycles, (b) magnified view of the interface boundary after three cycles (SEM magnification: 1000x).

The samples were then subjected to X-ray diffraction analysis with a wavelength of 54.1 Å, as shown in Fig. 8. The results indicate that no new phase or compound was formed. It is evident that during the ARB process in the fourth cycle, although accompanied by work hardening, minimal heat is generated, which is less than the activation energy required for the formation of intermetallic compounds.

Fig. 9 illustrates the changes in Vickers microhardness of the ARBed sample in different process cycles and annealed samples with and without nanoparticles. It is evident from the graph that microhardness increases in both cases by increasing the process cycles. At the end of the first cycle, the hardness value increases sharply from 71 HV in the annealed sample to 128 HV, mainly due to the high increase in dislocation density resulting from strain hardening. After the first cycle, the hardness increases with a lower slope, attributed to the reduction in strain hardening effects. Additionally, the microhardness remains almost constant in the final cycles due to the saturation of dislocation density and the disappearance of strain rate hardening effects. The Vickers microhardness value for ARBed aluminum at the end of the 4th cycle reaches its maximum value of 157 HV, which is more than twice than that of the initial sample.

During accumulative roll bonding of thin layers of 5083 aluminum with Al_2O_3 nanoparticles, strong mechanical and microstructural bonds are formed between the layers due to work hardening in the sheets, which increases interlayer adhesion. This is because during the rolling process, the layers of different metals are plastically deformed and interweaving. This mechanical interweaving prevents the layers from separating during loading and environmental conditions, and the surface irregularities caused by the Al_2O_3 nanoparticles contribute to an increase in the contact area between the layers and consequently an increase in the friction between them.

Table 3 compares the results obtained from the layer adhesion measurements for samples with and without nanoparticles in different cycles. The measured values in different cycles show that layer adhesion increases in both samples with/without nanoparticles with increasing cycles. Comparing the peel-off force of 25, 29, 31, and 37 N in samples without nanoparticles with
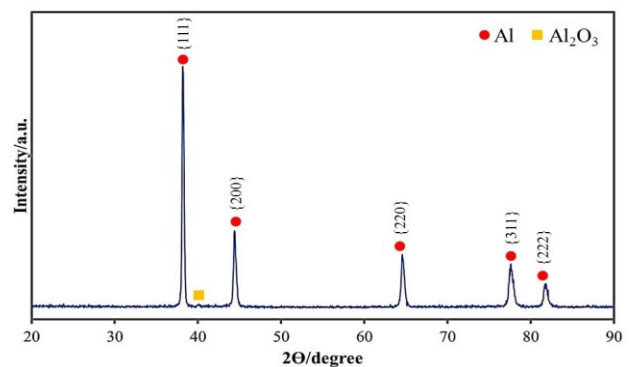

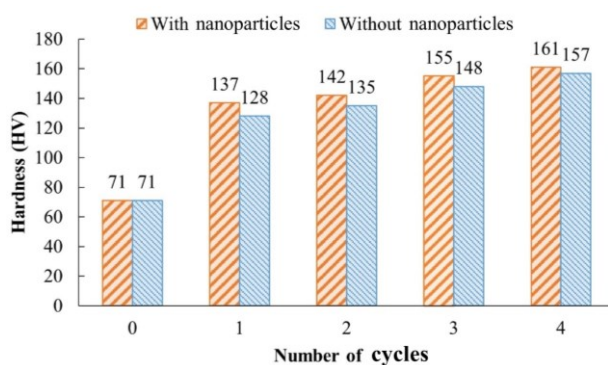**Fig. 8.** XRD pattern of Al_2O_3 nanocomposite in 4th cycle.

Fig. 9. Hardness graph in different cycles with nanoparticles and without nanoparticles.

forces of 28, 31, 35, and 41 N in samples with nanoparticles reveals an overall increase in adhesion due to the addition of nanoparticles. In the 4th cycle, the highest increase of approximately 11.9% is observed.

Table 3. Peeling adhesion between the layers with and without nanoparticles in different cycles

Type	1st cycle	2nd cycle	3rd cycle	4th cycle
With nanoparticle	27 N	32 N	35 N	42 N
Without nanoparticle	25 N	29 N	31 N	37 N
Difference (%)	7.4%	9.3%	11.4%	11.9%

4. Conclusion

In this study, the effects of applying Al_2O_3 nanoparticles between the layers in the accumulative roll bonding process of aluminum Al5083 sheets at room temperature were investigated in regards to the mechanical properties and interlayer adhesion of the laminated composite. The overall results are summarized as follows:

- With an increase in the number of cycles, the bonding force between the sheets increased from 37 N to 42 N over four cycles.
- Through the ARB process, the tensile strength of annealed sheets increased from 290 MPa to 421 MPa (in the first cycle), showing a considerable rate of increase.
- In the initial cycle of the ARB process, the elongation of the specimen relative to the

annealed sample rapidly decreased. Subsequently, with an increase in process cycles, the elongation rate decreased slightly compared to the previous cycle.

- The hardness of the sheets increased from 128 HV to 137 HV in the initial cycles using nanoparticles in this process. It remained relatively constant in the intermediate cycles and slightly decreased in the final cycles. The distribution of hardness throughout the thickness of the ARBed specimen is relatively uniform.
- The use of nanoparticles in the ARB process enhances tensile strength and hardness between aluminum layers while increasing the interlayer adhesion.

Conflict of Interest

The Authors declare that there is no conflict of interest.

Funding

Authors' Contributions

Mirshaban Jafari: Conceptualization, Methodology, Writing- Original Draft, Visualization. **S.M. Hossein Seyedkashi:** Project administration, Supervision, Writing- Review & Editing. **Majid Elyasi:** Supervision, Resources. **Yadollah Yaghoubinezhad:** Validation.

5. References

[1] Jamaati, R., & Toroghinejad, M. R. (2010). Effect of friction, annealing conditions and hardness on the bond strength of Al/Al strips produced by cold roll bonding process. *Materials & Design*, *31*(9), 4508-4513. https://doi.org/10.1016/j.matdes.2010.04.022

[2] Li, L., Nagai, K., & Yin, F. (2008). Progress in cold roll bonding of metals. *Science and Technology of Advanced Materials*, *9*(2), 023001. https://doi.org/10.1 088/1468-6996/9/2/023001

[3] Jamaati, R., & Toroghinejad, M. R. (2010). High-

strength and highly-uniform composite produced by anodizing and accumulative roll bonding processes. *Materials & Design*, *31*(10), 4816-4822. https://doi.org/10.1016/j.matdes.2010.04.048

[4] Shingu, P. H., Ishihara, K. N., Otsuki, A., & Daigo, I. (2001). Nano-scaled multi-layered bulk materials manufactured by repeated pressing and rolling in the Cu–Fe system. *Materials Science and Engineering: A*, *304*, 399-402. https://doi.org/10.1016/S0921-5093(00)01516-1

[5] Movchan, B. A., & Lemkey, F. D. (1997). Mechanical properties of fine-crystalline two-phase materials. *Materials Science and Engineering: A*, *224*(1-2), 136-145. https://doi.org/10.1016/S0921-5093(96)10455-X

[6] Chino, Y., Mabuchi, M., Kishihara, R., Hosokawa, H., Yamada, Y., Cui, E. W., Shimojima, K., & Iwasaki, H. (2002). Mechanical properties and press formability at room temperature of AZ31 Mg alloy processed by single roller drive rolling. *Materials Transactions*, *43*(10), 2554-2560. https://doi.org/10.2320/matertrans.43.25 54

[7] Pirgazi, H., Akbarzadeh, A., Petrov, R., & Kestens, L. (2008). Microstructure evolution and mechanical properties of AA1100 aluminum sheet processed by accumulative roll bonding. *Materials Science and Engineering: A*, *497*(1-2), 132-138. https://doi.org/10.1016/j.msea.2008.06.025

[8] Li, S., Beyerlein, I. J., Alexander, D. J., & Vogel, S. C. (2005). Texture evolution during multi-pass equal channel angular extrusion of copper: Neutron diffraction characterization and polycrystal modeling. *Acta Materialia*, *53*(7), 2111-2125. https://doi.org/10.1016/j.actamat.2005.01.023

[9] Richert, M., Liu, Q., & Hansen, N. (1999). Microstructural evolution over a large strain range in aluminium deformed by cyclic-extrusion–compression. *Materials Science and Engineering: A*, *260*(1-2), 275-283. https://doi.org/10.1016/S0921-5093(98)00988-5

[10] Khatibi, G., Horky, J., Weiss, B., & Zehetbauer, M. J. (2010). High cycle fatigue behaviour of copper deformed by high pressure torsion. *International Journal of Fatigue*, *32*(2), 269-278. https://doi.org/10.1016/j.ijfatigue.2009.06.017

[11] Fattah-Alhosseini, A., Naseri, M., & Alemi, M. H. (2016). Corrosion behavior assessment of finely dispersed and highly uniform Al/B4C/SiC hybrid composite fabricated via accumulative roll bonding process. *Journal of Manufacturing Processes*, *22*, 120-126. https://doi.org/10.1016/j.jmapro.2016.03.006

[12] Duan, J. Q., Quadir, M. Z., & Ferry, M. (2017). Engineering low intensity planar textures in commercial purity nickel sheets by cross roll bonding. *Materials Letters*, *188*, 138-141. https://doi.org/10.1016/j.matlet.2016.11.040

[13] Zeng, L. F., Gao, R., Fang, Q. F., Wang, X. P., Xie, Z. M., Miao, S., Hao, T. & Zhang, T. (2016). High strength and thermal stability of bulk Cu/Ta nanolamellar multilayers fabricated by cross accumulative roll bonding. *Acta Materialia*, *110*, 341-351. https://doi.org/10.1016/j.actamat.2016.03.034

[14] Eslami, A. H., Balali, M., & Seyedkashi, S. M. (2018). Study and comparison of simple shear extrusion and accumulative roll bonding processes in improving the mechanical and structural properties of copper. *Metallurgical Engineering*, *21*(2), 118-128. https://doi.org/10.22076/ME.2018.82259.1174

[15] Saito, Y., Utsunomiya, H., Tsuji, N., & Sakai, T. J. A. M. (1999). Novel ultra-high straining process for bulk materials—development of the accumulative roll-bonding (ARB) process. *Acta Materialia*, *47*(2), 579-583. https://doi.org/10.1016/S1359-6454(98)00365-6

[16] Dehghan, M., Qods, F., Gerdooei, M., & Mohammadian-Semnani, H. (2021). Influence of intermediate heating in cross accumulative roll-bonding process on planar isotropy of the mechanical properties of commercial purity aluminium sheet. *Metals and Materials International*, *27*, 4937-4951. https://doi.org/10.1007/s12540-020-00833-3

[17] Su, L., Lu, C., Li, H., Deng, G., & Tieu, K. (2014). Investigation of ultrafine grained AA1050 fabricated by accumulative roll bonding. *Materials Science and Engineering: A*, *614*, 148-155. https://doi.org/10.1016/j.msea.2014.07.032

[18] Bonnot, E., Helbert, A. L., Brisset, F., & Baudin, T. (2013). Microstructure and texture evolution during the ultra grain refinement of the Armco iron deformed by accumulative roll bonding (ARB). *Materials Science and Engineering: A*, *561*, 60-66. https://doi.org/10.1016/j.msea.2012.11.017

[19] Shaarbaf, M., & Toroghinejad, M. R. (2008). Nano-grained copper strip produced by accumulative roll bonding process. *Materials Science and Engineering: A*, *473*(1-2), 28-33. https://doi.org/10.1016/j.msea.2007.03.065

[20] Mehr, V. Y., Toroghinejad, M. R., & Rezaeian, A. (2014). The effects of oxide film and annealing treatment on the bond strength of Al–Cu strips in cold roll bonding process. *Materials & Design*, *53*, 174-181. https://doi.org/10.1016/j.matdes.2013.06.028

[21] Ng, H. P., Przybilla, T., Schmidt, C., Lapovok, R., Orlov, D., Höppel, H. W., & Göken, M. (2013).

Asymmetric accumulative roll bonding of aluminium–titanium composite sheets. *Materials Science and Engineering: A*, *576*, 306-315. https://doi.org/10.1016/j.msea.2013.04.027

[22] Gao, Y., Vini, M. H., & Daneshmand, S. (2022). Effect of nano Al2O3 particles on the mechanical and wear properties of Al/Al2O3 composites manufactured via ARB. *Reviews on Advanced Materials Science*, *61*(1), 734-743. https://doi.org/10.1515/rams-2022-0268

[23] Sedighi, M., Vini, M. H., & Farhadipour, P. (2016). Effect of alumina content on the mechanical properties of AA5083/Al2O3 composites fabricated by warm accumulative roll bonding. *Powder Metallurgy and Metal Ceramics*, *55*, 413-418. https://doi.org/10.1007/s11106-016-9821-0

[24] Mosleh-Shirazi, S., Akhlaghi, F., & Li, D. Y. (2016). Effect of SiC content on dry sliding wear, corrosion and corrosive wear of Al/SiC nanocomposites. *Transactions of Nonferrous Metals Society of China*, *26*(7), 1801-1808. https://doi.org/10.1016/S1003-6326(16)64294-2

[25] Mosleh-Shirazi, S., & Akhlaghi, F. (2019). Tribological behavior of Al/SiC and Al/SiC/2 vol% Gr nanocomposites containing different amounts of nano SiC particles. *Materials Research Express*, *6*(6), 065039.

[26] Lee, J. M., Lee, B. R., & Kang, S. B. (2005). Control of layer continuity in metallic multilayers produced by deformation synthesis method. *Materials Science and Engineering: A*, *406*(1-2), 95-101. https://doi.org/10.1016/j.msea.2005.06.030

[27] Yazar, Ö., Ediz, T., & Öztürk, T. (2005). Control of macrostructure in deformation processing of metal/metal laminates. *Acta Materialia*, *53*(2), 375-381. https://doi.org/10.1016/j.actamat.2004.09.033

[28] Sadoun, A. M., Meselhy, A. F., & Deabs, A. W. (2020). Improved strength and ductility of friction stir tailor-welded blanks of base metal AA2024 reinforced with interlayer strip of AA7075. *Results in Physics*, *16*, 102911. https://doi.org/10.1016/j.rinp.2019.102911

[29] Xu, R., Liang, N., Zhuang, L., Wei, D., & Zhao, Y. (2022). Microstructure and mechanical behaviors of Al/Cu laminated composites fabricated by accumulative roll bonding and intermediate annealing. *Materials Science and Engineering: A*, *832*, 142510. https://doi.org/10.1016/j.msea.2021.142510

[30] Sadoun, A. M., Abd El-Wadoud, F., Fathy, A., Kabeel, A. M., & Megahed, A. A. (2021). Effect of through-the-thickness position of aluminum wire mesh on the mechanical properties of GFRP/Al hybrid composites. *Journal of Materials Research and Technology*, *15*, 500-510. https://doi.org/10.1016/j.jmrt.2021.08.026

[31] Chen, Y., Nie, J., Wang, F., Yang, H., Wu, C., Liu, X., & Zhao, Y. (2020). Revealing hetero-deformation induced (HDI) stress strengthening effect in laminated Al-(TiB2+ TiC) p/6063 composites prepared by accumulative roll bonding. *Journal of Alloys and Compounds*, *815*, 152285. https://doi.org/10.1016/j.jallcom.2019.152285

[32] Liu, C. Y., Wang, Q., Jia, Y. Z., Zhang, B., Jing, R., Ma, M. Z., Jing, Q., & Liu, R. P. (2012). Effect of W particles on the properties of accumulatively roll-bonded Al/W composites. *Materials Science and Engineering: A*, *547*, 120-124. https://doi.org/10.1016/j.msea.2012.03.095

[33] Saito, Y., Tsuji, N., Utsunomiya, H., Sakai, T., & Hong, R. G. (1998). Ultra-fine grained bulk aluminum produced by accumulative roll-bonding (ARB) process. *Scripta Materialia*, *39*(9), 1221-1227. https://doi.org/10.1016/S1359-6462(98)00302-9